Smart Structures and Systems, *Vol. 24, No. 3 (2019) 319-332*
DOI: https://doi.org/10.12989/sss.2019.24.3.319

Online automatic structural health assessment of the Shanghai Tower

Qilin Zhang, Xiaoxiang Tang, Jie Wu* and Bin Yang

College of Civil Engineering, Tongji University, 1239 Siping Road, Shanghai 200092, PR China

(Received November 13, 2018, Revised June 14, 2019, Accepted July 11, 2019)

Abstract. Structural health monitoring (SHM) is of great importance to super high-rise buildings. The Shanghai Tower is currently the tallest building in China, and a complete SHM system was simultaneously constructed at the beginning of the construction of the tower. Due to the variety of sensor types and the large number of measurement points in the SHM system, an online automatic structural health assessment method with few computations and no manual intervention is needed. This paper introduces a structural health assessment method for the Shanghai Tower that uses the coefficients of an autoregressive (AR) time series model as structural state indicators. An analysis of collected data indicates that the coefficients of the AR model are affected by environmental factors, and the principal component analysis method is used to remove the influence of environmental factors. Finally, the control chart method is used to track the changes in structural state indicators, and a plan for online automatic structure health state evaluation is proposed. This method is applied to long-term acceleration and inclination data from the Shanghai Tower and successfully identifies the changes in the structural state. Overall, the structural state indicators of the Shanghai Tower are stable, and the structure is in a healthy state.

Keywords: structural health assessment; structural health monitoring; principal component analysis; Shanghai Tower; online automatic system

1. Introduction

With economic development, increasing numbers of super high-rise buildings have been built around the world. Super high-rise buildings generally have a long service life, and as time goes on, the carrying capacity of such structures inevitably decreases. Therefore, structural health monitoring (SHM) and health assessment are extremely important. Many existing and newly built super high-rise buildings, such as the Burj Khalifa (Abdelrazaq *et al*. 2013), the Shanghai World Financial Center (Shi *et al*. 2012), the Canton Tower (Ni *et al*. 2009, Yi *et al*. 2015) and the Tianjin 117 Tower (Liu *et al*. 2016), are equipped with SHM systems. An SHM system usually consists of several subsystems, including a sensor system, a data acquisition and transmission system, a data management system, and a structural health assessment system. Among these subsystems, the most important is the structural health assessment system.

In the methods for structural health assessment, the dynamic characteristics of structures are typically used as indicators of the structural state, especially the modal parameters. Such methods are based on the assumption that changes in the structural state are reflected by the dynamic characteristics of structures. However, most studies have noted that modal parameters are affected by environmental factors. Cornwell *et al*. (1999) studied the variability in the modal properties of the Alamosa Canyon Bridge in southern New Mexico. Peeters (2001) studied the environmental effects on the modal parameters of the Z24-bridge during a one-year monitoring period and showed that changes in the vibration response resulting from damage can be separated from changes resulting from environmental variability. Yan *et al*. (2005a, b) proposed the use of principal component analysis (PCA) to remove the influence of environmental factors. In addition, the traditional modal parameter identification methods require human intervention, which make such methods difficult to use for online automatic structural health assessments. Therefore, some scholars have proposed fully automatic modal parameter identification methods. Magalhães *et al*. (2009) proposed a method based on covariance-driven stochastic subspace identification (SSI) and hierarchical clustering and applied the method to monitor a concrete arch bridge for two months. Reynders *et al*. (2012) proposed an automatic modal parameter identification method based on stochastic subspace identification and clustering methods and validated the method with monitoring data from the Z24-bridge. Ubertini *et al*. (2013) proposed an automated modal identification procedure classified as an SSI technique based on clustering analysis. This method was applied in operational analyses of two bridges. In addition, this method was later applied in the long-term SHM of a historical bell tower in Italy (Ubertini *et al*. 2016).

The automatic modal parameter identification methods based on clustering work well but are associated with high computational complexity. Sohn (2001) proposed that a time series model can be used to fit vibration data and that obtained time series model coefficients can reflect the dynamic characteristics of a structure. This method avoids the identification of modal parameters, requires no human

*Corresponding author, Ph. D.
E-mail: wwujie@tongji.edu.cn

 ISSN: 1738-1584 (Print), 1738-1991 (Online)

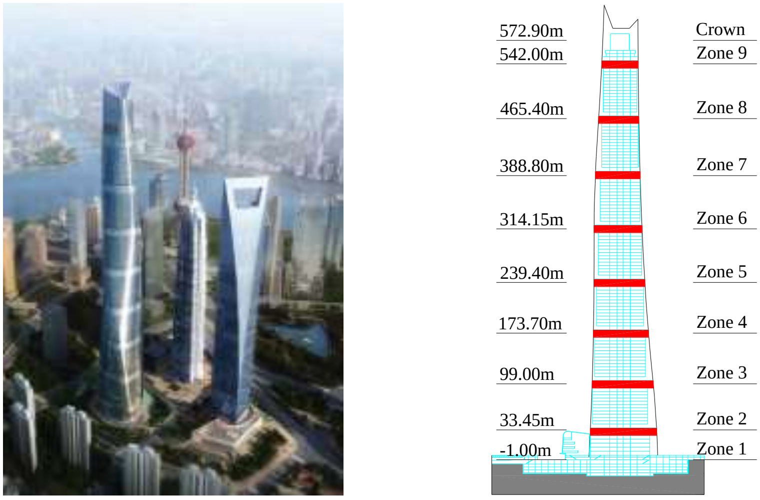

Fig. 1 The Shanghai Tower

intervention, eliminates the cluster analysis steps and greatly reduces the number of calculations. A series of subsequent studies verified the feasibility of the method. Lu (2005) applied the auto-regressive with exogenous input time series model to diagnose structural damage and verified the model with numerical examples. Nair *et al.* (2006) applied a time series algorithm to obtain analytical and experimental results for an ASCE benchmark structure and found that the algorithm identified minor to severe damage at the local scale, as defined for the benchmark structure. In addition, de Lautour (2010) treated the coefficients of AR models as damage-sensitive features and showed that the combination of AR models and an artificial neural network was an efficient approach for damage classification and estimation based on experimental data from a 3-story structure and the ASCE Phase II Experimental SHM benchmark structure. Posenato *et al.* (2008) tested a time series method considering numerically simulated elements with sensors and a range of damage severities. The method demonstrated superior performance compared to traditional methods in identifying the state change of structure.

Based on previous studies, this paper uses the AR model to fit the acceleration and inclination data from the Shanghai Tower. The data indicate that the environmental factors influence the coefficients of the AR model. Therefore, PCA is used to remove the influence of environmental factors on the coefficients of the AR model, and the control chart method is used to track the PCA reconstruction error for the coefficients of the AR model. As described above, an online automatic structural health assessment method for the Shanghai Tower is established. This method effectively indicated the structural state change caused by the damper lock during the damper test period of the Shanghai Tower in May 2016 and confirmed that the Shanghai Tower is in a healthy state.

This article mainly includes the following sections: an overview of the Shanghai Tower; an introduction to the proposed online automatic structural health assessment method, which is based on time series analysis; an outline of PCA and the control chart method; and the application of the online automatic structural health assessment method at the Shanghai Tower.

2. Overview of the Shanghai Tower

2.1 Architectural and structural forms

The Shanghai Tower, which is located in the Lujiazui Financial Center on the banks of the Huangpu River, was completed at the end of 2015 and is currently the tallest building in China (see Fig. 1). As discussed by Zhang *et al.* (2015), the building is a multipurpose skyscraper that mainly includes public facilities, such as offices, hotels, businesses, and tourist attractions. The tower has 124 floors above ground level, with a building height of 632 m. The tower is divided into 8 sections and a sightseeing layer in the vertical direction (see Figs. 1 and 2). The podium is 7 floors above ground level, with a building height of 38 m and a basement of five floors. The foundation of the building is a piled raft foundation. The main structure adopts a mega-frame outrigger core tube system that consists of a reinforced concrete core tube, a mega-frame and an outrigger truss. The outer surface of the building is composed of a glass curtain wall. The plane shape is a chamfered triangle, and it is rotated clockwise by 120 degrees along the height of the building to form the curved surface of the building and provide good resistance to wind loads.

2.2 The structural health monitoring system

Due to the importance of the Shanghai Tower, a complete SHM system (Su *et al.* 2013) was deployed by the cooperation of Tongji University, Hong Kong Polytechnic University and Tongji Architectural Design (Group) Co. Ltd. The SHM system consists of the following four parts: a sensor system, a data acquisition and transmission system, a

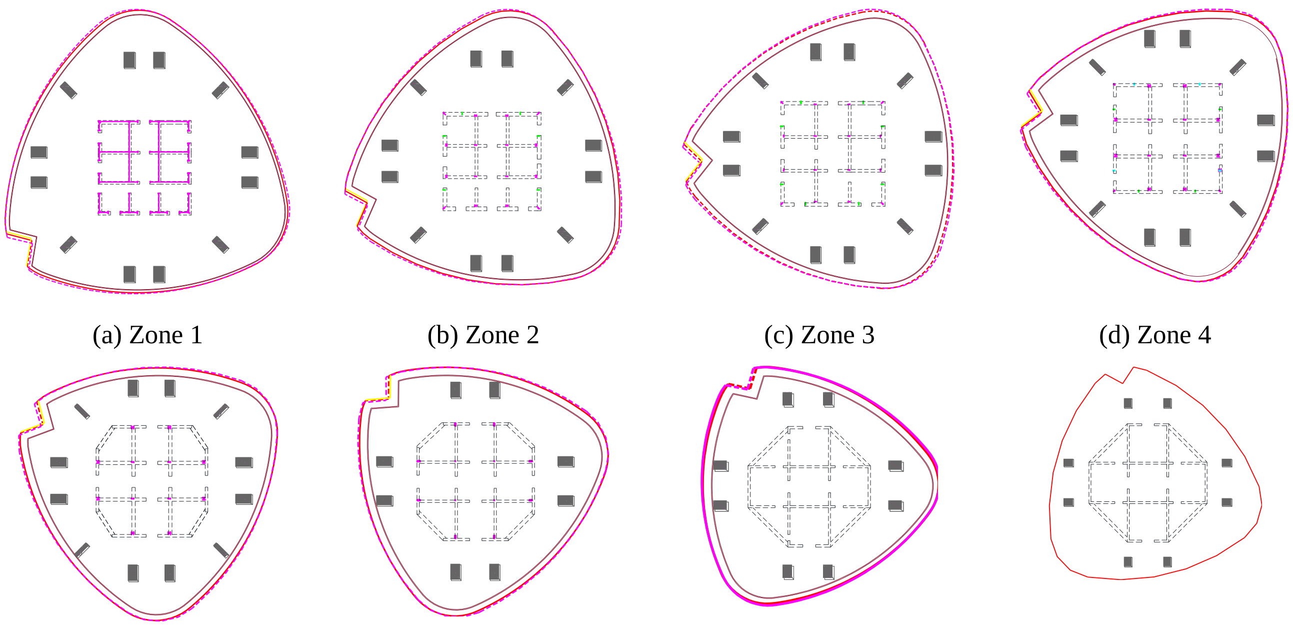

(a) Zone 1 (b) Zone 2 (c) Zone 3 (d) Zone 4

(e) Zone 5 (f) Zone 6 (g) Zone 7 (h) Zone 8

Fig. 2 Structural layout of typical floors in each zone

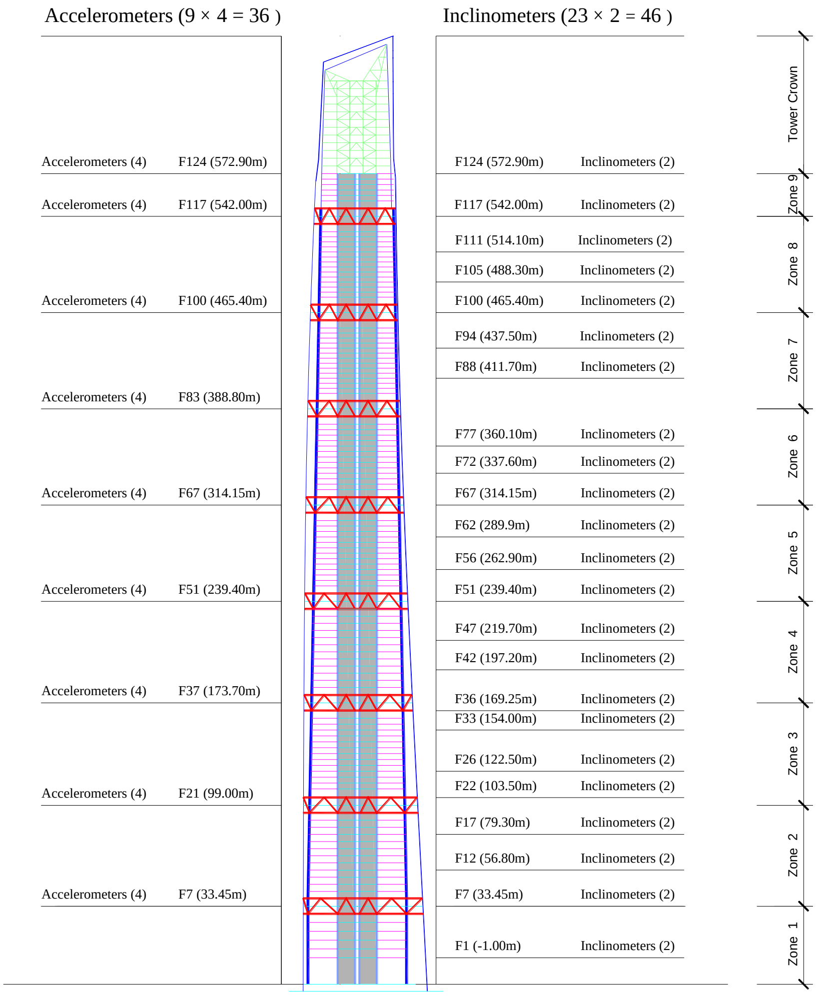

Fig. 3 Vertical layout of the inclinometers and accelerometers

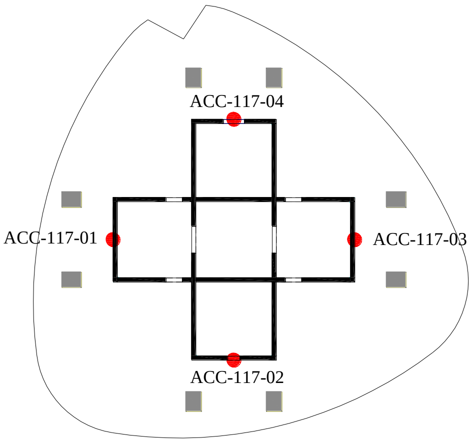

(a) accelerometers

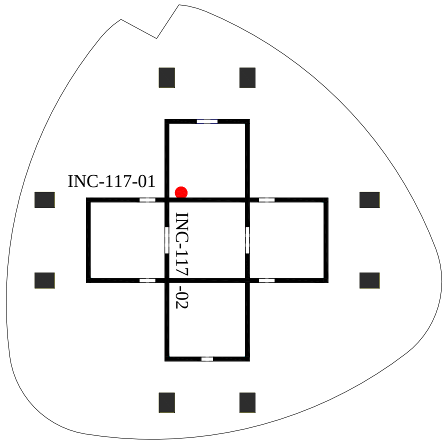

(b) inclinometers

Fig. 4 Horizontal layout of inclinometers and accelerometers in a typical floor

Table 1 Comparison of the modal frequencies obtained from the FEA and AVT (Hz)

		f_{x1}	f_{y1}	f_{t1}	f_{y2}	f_{x2}
FEA (Ding *et al.* 2010)	ETABS	0.110	0.112	0.179	0.306	0.318
	ABAQUS	0.110	0.111	0.243	0.324	0.328
	ANSYS	0.110	0.111	0.217	0.319	0.324
AVT	Acceleration	0.107	0.109	0.214	0.314	0.325
	Inclination	0.107	0.108	—	0.322	0.325

data storage system, and a structural health assessment system.

The sensor system is used to measure environmental factors and the response of the structure, and it includes 2 anemometers with acquisition sampling rate (ASR) of 100 Hz, 55 temperature sensors with ASR of 1/60 Hz, 27 wind pressure gauges with ASR of 100 Hz, 36 accelerometers with ASR of 100 Hz, 46 inclinometers with ASR of 100 Hz, 27 wind vibration sensors with ASR of 100 Hz, 183 strain gauges with ASR of 1/60 Hz, 18 welding crack sensors with ASR of 1/60 Hz, 2 seismographs, and 2 GPS sensors. The vertical layouts of accelerometers and inclinometers are shown in Fig. 3, and the horizontal layouts of the accelerometers and inclinometers in a typical floor (117^{th} floor) are shown in Fig. 4.

The data acquisition and transmission system consists of 11 data collection substations along the height of the building. This system is responsible for collecting the data from each sensor in the section and transmitting the collected data to the data acquisition terminal in the underground 1st floor through optical fibers.

The data storage system stores and manages the data collected by the data acquisition terminal through a database management system and periodically backs up the collected data to cloud storage.

The structural health state assessment system acquires the dynamic characteristics of the structure based on the collected data, establishes health state indicators for the structure, and evaluates and tracks the health state of the structure.

2.3 Finite element analysis

To obtain the dynamic characteristics of the Shanghai Tower, several finite element (FE) models of the tower were established by different FE software during the structural design phase by Tongji Architectural Design (Group) Co. Ltd. The dynamic characteristics obtained from the finite element models can be used as a reference for those obtained from the measurement data. The first five modal frequencies of the Shanghai Tower obtained by finite element analysis (FEA) (Ding *et al*. 2010) and an ambient vibration test (AVT) are shown in Table 1.

2.4 Ambient vibration test

In the SHM of civil buildings, the ambient excitations are immeasurable; therefore, modal parameter identification is based on output-only methods. In this paper, the peak picking method is chosen to identify the modal frequencies of the Shanghai Tower. The basic theory of the peak picking method is shown in Eq. (1)

$$G_y(j\omega) = \overline{H}(j\omega)G_x(j\omega)H(j\omega)^T \tag{1}$$

where $G_x(j\omega)$ is the power spectral density (PSD) of the input signal, $H(j\omega)$ is the transfer function, and $G_y(j\omega)$ is the PSD of the output signal.

In general, the ambient input has white noise-like characteristics, and the PSD function $G_x(j\omega)$ is a constant. Therefore, the peak value of $G_y(j\omega)$ (the PSD function of

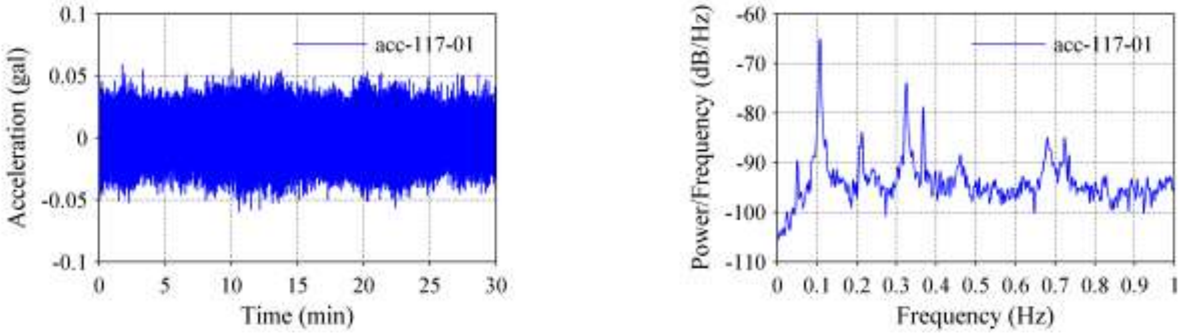

(a) sample acceleration data (b) PSD

Fig. 5 Measurement point acc-117-01

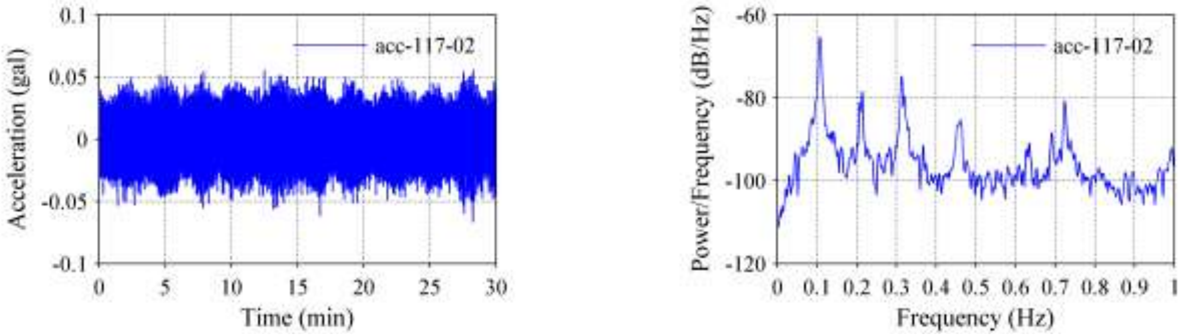

(a) sample acceleration data (b) PSD

Fig. 6 Measurement point acc-117-02

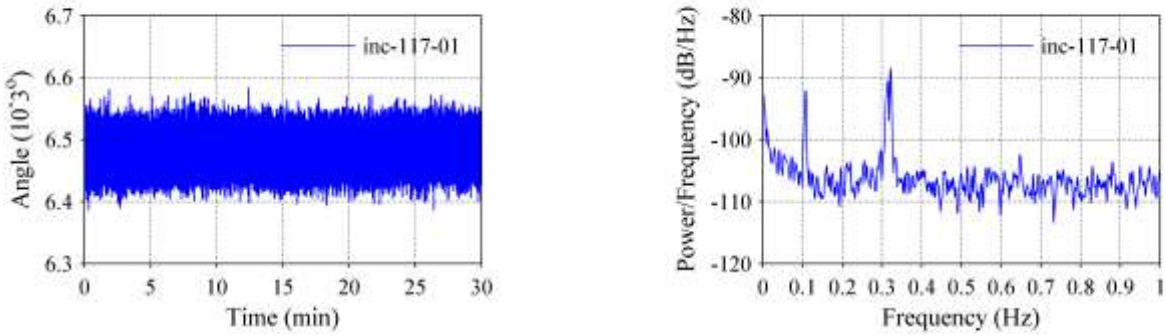

(a) sample angle data (b) PSD

Fig. 7 Measurement point inc-117-01

the output signal) is in accordance with the transfer function $H(j\omega)$, and the peak value of $G_y(j\omega)$ can be used to identify the characteristic frequencies.

The PSD is estimated by using the function pwelch() in Matlab software based on the Welch's method. The discrete-time signal vector of acceleration and inclination is divided into eight sections with 50% overlap, and each section is windowed with a Hamming window and eight modified periodograms are computed and averaged. In addition, the number of FFT points is 32678. The 30-minute acceleration time history curve and the corresponding PSD curve of the 117th floor in the X and Y directions are shown in Figs. 5 and 6, respectively. The 30-minute inclination time history curve and the corresponding PSD curve of the 117th floor in the X and Y directions are shown in Figs. 7 and 8, respectively.

Table 1 shows that the modal frequencies obtained from the FEM and the AVT. The frequencies obtained by AVT are basically consistent with those obtained by FEM. This finding indicates that the response data acquired by the SHM system are accurate and can be used for further analysis. Moreover, the inclination data can also be used to

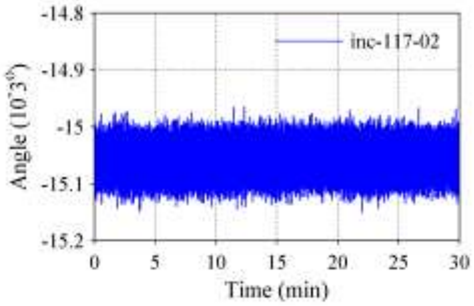

(a) sample angle data

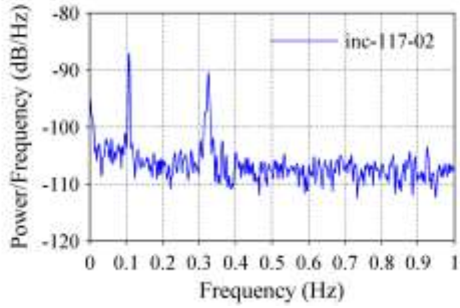

(b) PSD

Fig. 8 Measurement point inc-117-02

follows

identify the modal frequencies, but the torsional mode cannot be well identified.

3. Online automatic structural health assessment method

Due to the variety of sensor types and the large number of measurement points in the SHM system of the Shanghai Tower, an online automatic structural health assessment method with limited computations and no manual intervention is needed. This paper proposes an online automatic health assessment method based on the combination of time series model, PCA and the control chart method.

Based on previous research, the coefficients of the AR model can be used to reflect the dynamic characteristics of the structure. Therefore, we use the coefficients of the AR model as indicators to characterize the dynamic characteristics of the structure. However, an analysis of the measured data revealed that the coefficients of the AR model can be affected by environmental factors. Thus, PCA is utilized to analyze the coefficients of the AR model, and the principal components that reflect the influence of environmental factors can be obtained. The coefficients of the AR model are reconstructed using the acquired principal components, and the reconstruction error reflects the state of the structure with the influence of environmental factors eliminated. Finally, the control chart method is used to automatically monitor and track the health status of the structure based on the reconstruction error.

3.1 Time series analysis

The time series-based structural health assessment methods directly use the structural vibration signal to fit a time series model. Then, the coefficients of the time series model are used as structural state indicators to assess the structural health state. The assessment process does not require time-frequency domain transform, nor does it depend on the structural model; thus, it is suitable for the continuous online monitoring of structures.

For a time series of observations, there is a certain correlation among the observations in the sample. The model used to describe this time series can be expressed as

$$x_t = f(x_{t-1}, x_{t-2}, \dots) + a_t \tag{2}$$

where $f(\cdot)$ is a function that relates the observation x_t to $x_{t-1}, x_{t-2}, \dots$. and can be obtained by time series analysis. a_t is the modeling error produced when $f(\cdot)$ is used to describe x_t. It is generally assumed that a_t is Gaussian white noise with a mean of zero and a constant variance.

Autoregressive moving average (ARMA) model is the basic time series model which have variation forms of AR and MA. For a stationary, normal, zero-mean time series $\{x_t\}\,(t = 1, 2, \dots, N)$, the ARMA model can be expressed as follows

$$x_t - \sum_{i=1}^{n} \phi_i x_{t-i} = a_t - \sum_{j=1}^{m} \theta_j a_{t-j} \tag{3}$$

where ϕ_i is the autoregressive coefficient, which indicates the degree of influence of x_{t-i} on x_t, and θ_j is the moving average coefficient, which indicates the degree of influence of a_{t-j} on x_t.

Now, the post-shift operators B and C, where $B^i x_t = x_{t-i}$ and $C^j a_t = a_{t-i}$, can be introduced, and equation (3) can be reformulated as follows.

$$\left(1 - \sum_{i=1}^{n} \phi_i B^i\right) x_t = \left(1 - \sum_{j=1}^{m} \theta_j C^j\right) a_t \tag{4}$$

If we denote $\phi(B) = (1 - \sum_{i=1}^{n} \phi_i B^i)$ and $\theta(C) = (1 - \sum_{j=1}^{m} \theta_j C^j)$, then equation (3) can be simplified as

$$x_t = \theta(C)/\phi(B)\, a_t. \tag{5}$$

Eq. (5) shows that if a_t is the input and x_t is the output, the ARMA model describes a system with a transfer function of $\theta(C)/\phi(B)$. Under the principle of output equivalence, the system is an actual physical equivalent system with white noise as the input and x_t as the output. In the equation, $\phi(B)$ characterizes the inherent characteristics of the system, and $\theta(C)$ characterizes the connection between the system and the outside world.

In Eq. (3), when $\theta_j = 0$, there is no moving average portion of the model, and the ARMA model becomes an AR model that which can be expressed as follows.

$$x_t - \sum_{i=1}^{n} \phi_i x_{t-i} = a_t \tag{6}$$

Eq. (6) is called an n-order AR model and is denoted as AR(n). Because the AR model does not contain the moving average part of the ARMA model, the coefficients are linearly estimated. The calculation is simple and rapid and has obvious advantages in engineering applications, such as in fault diagnosis, structure monitoring, and online control. In the following section, the AR model is used to model time series of acceleration and inclination data from the Shanghai Tower.

3.2 Primary component analysis

According to time series theory, the coefficients of the AR model of the structural vibration response reflect the state of the structure itself. However, based on an analysis of the data obtained from the actual monitoring of the Shanghai Tower, the environmental factors also have a certain influence on the coefficients of the AR model. The purpose of PCA is to obtain the principal components that have a large effect on the coefficients of the AR model. These principal components reflect the influence of environmental factors. If the principal components are properly selected, the PCA reconstruction error of the coefficients of the AR model will not include the influence of environmental factors.

PCA (Jolliffe 2011) was first proposed by Carl Pearson in 1901. The method involves performing singular value decomposition on the covariance matrix of the data to obtain the feature vectors and feature values. The feature vectors are arranged according to the magnitude of the weights (the contribution of each feature vector to the variance) from large to small. In the general analysis, the first few feature vectors with a cumulative variance contribution greater than 85% are considered as the principal components. In the analysis of monitoring data from the Shanghai Tower, the principal components reflect the influence of environmental factors on the coefficients of the time series model. The illustration of PCA is as follows.

$\boldsymbol{x_i} \in \mathbb{R}^{\boldsymbol{n}}$ is a sample vector of AR model coefficients. In the training phase, N samples are used to form the AR model coefficient matrix $\boldsymbol{X}$, where $\boldsymbol{X} = [\boldsymbol{x_1}, \boldsymbol{x_2}, \cdots, \boldsymbol{x_N}]$.

Additionally, $\boldsymbol{X} \in \mathbb{R}^{n \times N}$, where n is the order of the AR model and N is the number of samples.

A covariance matrix of $\boldsymbol{X}$ is established, and singular value decomposition is performed on the matrix.

$$\boldsymbol{X}\boldsymbol{X}^T = \boldsymbol{U}\boldsymbol{\Lambda}\boldsymbol{U}^T \tag{8}$$

In Eq. (8), $\boldsymbol{U}$ is an $n \times n$ feature vector matrix, and $\boldsymbol{U}\boldsymbol{U}^T = I, \boldsymbol{\Lambda}$ is the diagonal matrix formed by the feature values.

$$\boldsymbol{\Lambda} = \begin{bmatrix} \lambda_1 & 0 & \dots & 0 \\ 0 & \lambda_2 & \dots & 0 \\ \vdots & \vdots & \ddots & \vdots \\ 0 & 0 & \dots & \lambda_n \end{bmatrix} \tag{9}$$

According to the feature vector matrix and a parameter sample $\boldsymbol{x_i}$ of the original AR model, the following relation can be obtained

$$\boldsymbol{y_i} = \boldsymbol{U}^T \boldsymbol{x_i} \tag{10}$$

where $\boldsymbol{y_i}$ is a vector in the feature vector space and every member of the vector is the magnitude in the feature vector direction. The amount of information associated with the original variable for each feature vector is represented by $\beta_i = \lambda_i / \sum_{i=1}^{n} \lambda_i$; therefore, $\sum_{i=1}^{m} \beta_i$ is the cumulative variance contribution of the first m feature vectors. The number of principal components can be determined according to the cumulative variance contribution of feature vectors. In the selection of the principal component, the first m feature vectors with a cumulative variance contribution greater than 85% can be selected in most cases. The matrix formed by the principal components is denoted as $\widehat{U}$.

The reconstruction of vector $\boldsymbol{x_i}$, can be expressed as follows.

$$\widehat{\boldsymbol{x}}_i = \widehat{\boldsymbol{U}}\, \widehat{\boldsymbol{U}}^T \boldsymbol{x_i} \tag{11}$$

Moreover, the reconstruction error vector $\boldsymbol{e_i}$ can be obtained by Eq. (12).

$$\boldsymbol{e_i} = \boldsymbol{x_i} - \widehat{\boldsymbol{x}}_{\boldsymbol{i}} \tag{12}$$

3.3 Control chart method

In the analysis above, it is clear that the PCA reconstruction error $\boldsymbol{e_i}$ of the AR model coefficients can be used as a structural state indicator. The structural state change will cause the probability distribution of the reconstruction error $\boldsymbol{e_i}$ to change; therefore, after $\boldsymbol{e_i}$ is obtained, the state change can be determined by the abnormal distribution of the reconstruction error. The magnitude of the reconstruction error $\boldsymbol{e_i}$ is measured using the Euclidean distance. Changes in the magnitude of $\boldsymbol{e_i}$ are tracked using the control chart method. The illustration of the control chart method is shown in Fig. 9.

The application of the control chart method is divided into two phases: the initial phase and the operation phase. In the initial phase, the structure is considered to be in a healthy state. The SHM system acquires a large amount of data in this phase. The vibration data are periodically fitted by the AR model to determine the coefficients of the AR model, and PCA is performed with the coefficients. After obtaining the principal components, the coefficients of the AR model are reconstructed to obtain the statistical distribution of the Euclidean distance of the reconstruction error. In the operation phase, for the coefficients of the AR model obtained by the new observations, the principal components obtained in the initial phase are used to reconstruct the coefficients of the model, and the reconstruction error is then obtained.

The magnitude of the reconstruction error $\boldsymbol{e_i}$ is denoted as d_i, and d_i is always greater than 0; thus, the lower control limit is 0. The upper control limit (UCL) is determined by statistical methods and corresponds to the 95% cumulative probability distribution. Points that exceed the UCL are deemed outliers. Tracking the d_i value, if

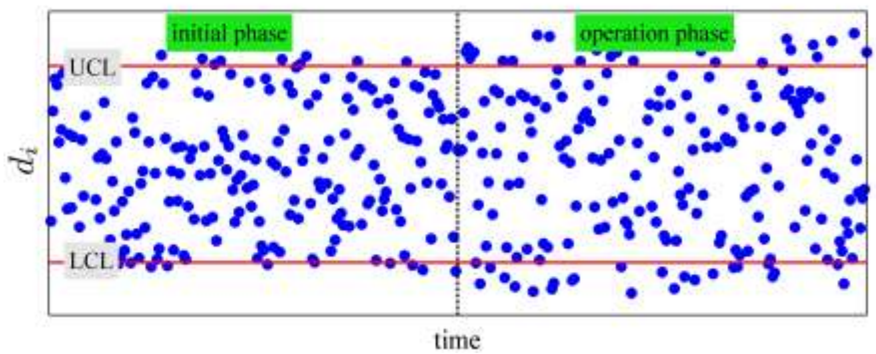

Fig. 9 Illustration of the control chart method

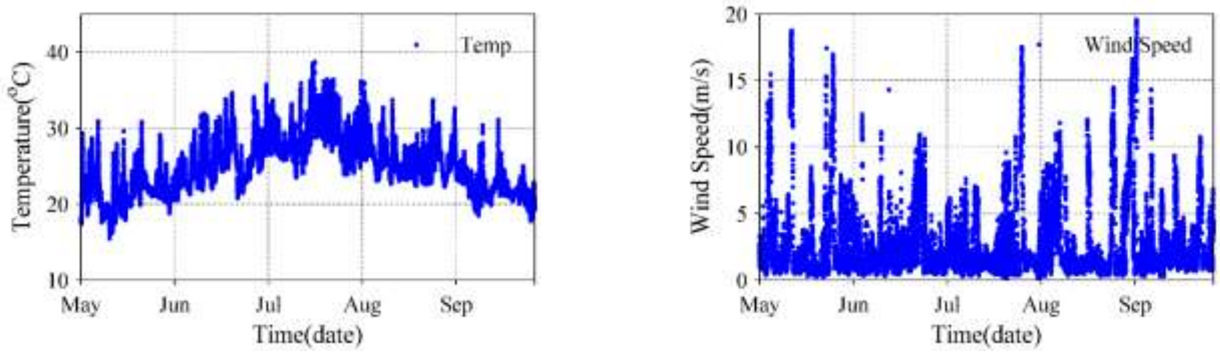

(a) temperature (b) wind speed

Fig. 10 Time histories of the 10-minute-averaged temperature and wind speed

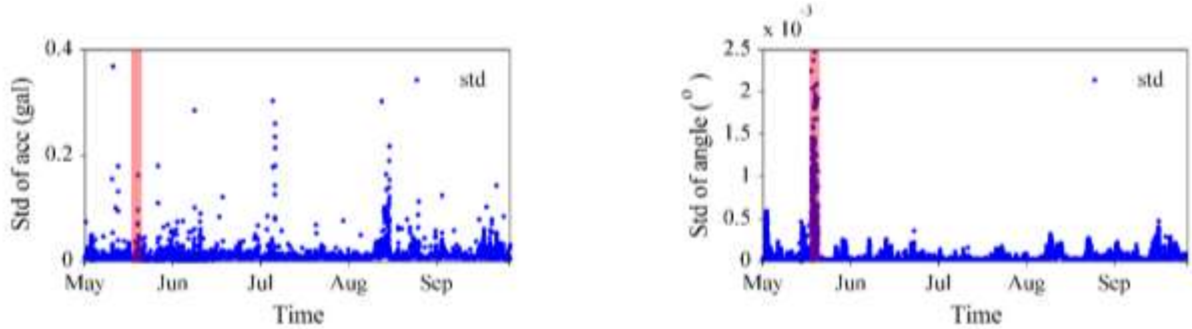

(a) acceleration (b) inclination

Fig. 11 Time histories of the standard deviation of acceleration and inclination

the unit time span (such as weekly) percentage of outliers is greater than 5% and lasts for a long time, the structure may be in an unhealthy state, and further inspection is required.

4. Structural health assessment of the Shanghai Tower

In the SHM system of the Shanghai Tower, to measure the response of the main structure under environmental excitation, accelerometers and inclinometers are arranged on the key floors to measure the vibration and inclination of the main structure. The data sampling frequency is 100 Hz for both acceleration and inclination measurements. In the following analysis, the acceleration and inclination data from the 117^{th} floor are analyzed using the method proposed above. The time span of the monitoring data analyzed in this paper ranges from May 1, 2016, to September 24, 2016.

During the data analysis period, the time history curve of the 10-minute-averaged temperature is shown in Fig. 10(a), and the temperature varies from 15 degrees Celsius to 38 degrees Celsius. The time history curve of the 10-

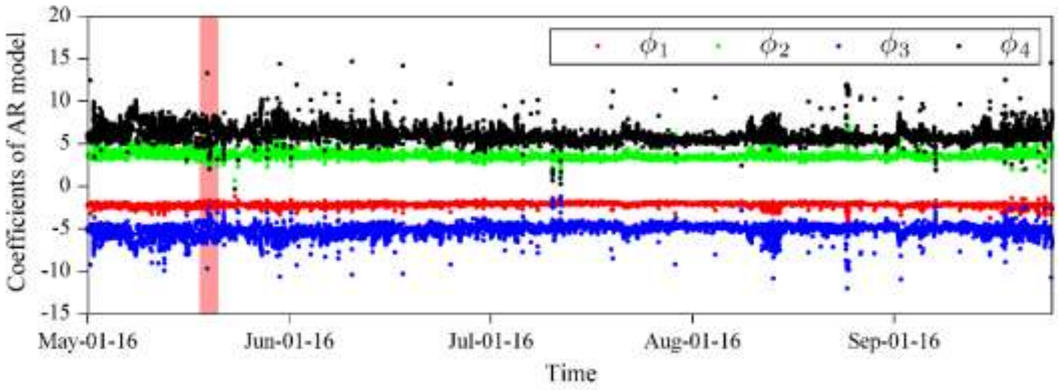

Fig. 12 Time histories of the first four AR model coefficients of acceleration on the 117th floor

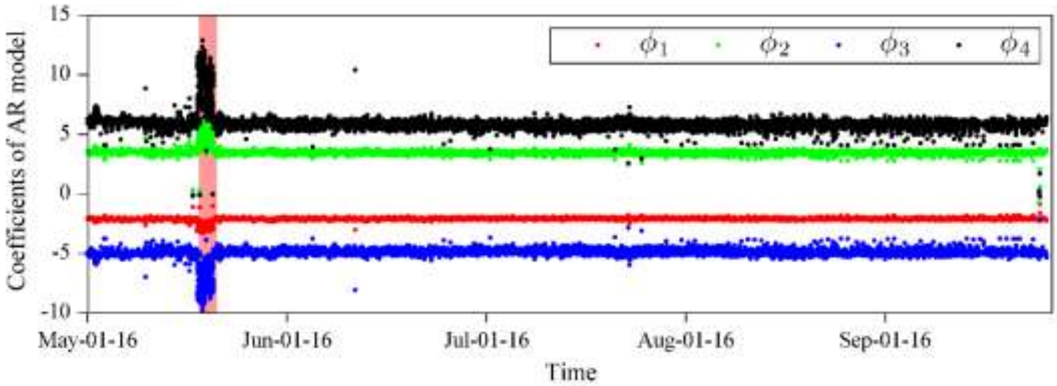

Fig. 13 Time histories of the first four AR model coefficients of inclination on the 117th floor

minute-averaged wind speed is also shown in Fig. 10(b). Since the data analysis period is mainly in the summer, the main distribution of the wind direction is between 180 and 270 degrees, which is a southeast wind (the wind direction angle definition of the anemometers on Shanghai Tower is 0 degrees north, and the angle increases in the counterclockwise direction). Since the distribution of wind direction angles is relatively concentrated, in the analysis of the correlation between the AR model parameters and the wind speed, the corresponding correlation coefficient is calculated using the total wind speed to simplify the calculations.

During the data analysis period, the 10-minute standard deviations of the X-direction acceleration and inclination time histories on the 117^{th} floor are shown in Fig. 11. The standard deviation of the inclination significantly increased in mid-May, and abnormal state lasted about three days. This increase occurred because the damper of the Shanghai Tower was tested in mid-May, and the damper was locked during the test, which caused a change in the dynamic characteristics of the structure. The standard deviation of the inclination reflects a change in the dynamic structural characteristics. However, changes in the dynamic structural characteristics were not reflected in the standard deviation of acceleration.

4.1 Environmental effects on AR model coefficients

According to the autocorrelation and partial autocorrelation analyses of the acceleration and inclination time history data, the AR model can be used to model the time series of acceleration and inclination data. According to the AIC criterion (Akaike 1973), the order of the AR model is determined to be 30.

For the collected acceleration and inclination data, AR model fitting is performed every 10 minutes to obtain the corresponding model coefficients. Then, the time history curves of the AR model coefficients can be obtained. In the data analysis period in this paper, the time history curves of the first four AR model coefficients of acceleration and inclination in the X direction on the 117^{th} floor are shown in Figs. 12 and 13, respectively. Due to the damper test in mid-May, the AR model coefficients of inclination displayed obvious variations around May 17. However, the AR model coefficients of acceleration did not significantly change during the damper test.

The correlation analysis results in Table 2 indicate that the AR model coefficients of acceleration have a certain degree of correlation with the temperature, and there is no obvious correlation with the wind speed. There is no significant correlation between the AR model coefficients

Table 2 Correlation coefficients between the first four AR model coefficients and environmental factors

	Acceleration				*Inclination*			
	ϕ_1	ϕ_2	ϕ_3	ϕ_4	ϕ_1	ϕ_2	ϕ_3	ϕ_4
Temperature	0.207	-0.157	0.149	-0.147	0.143	-0.079	0.083	-0.085
Wind speed	-0.161	0.134	-0.134	0.129	-0.067	0.036	-0.048	0.042

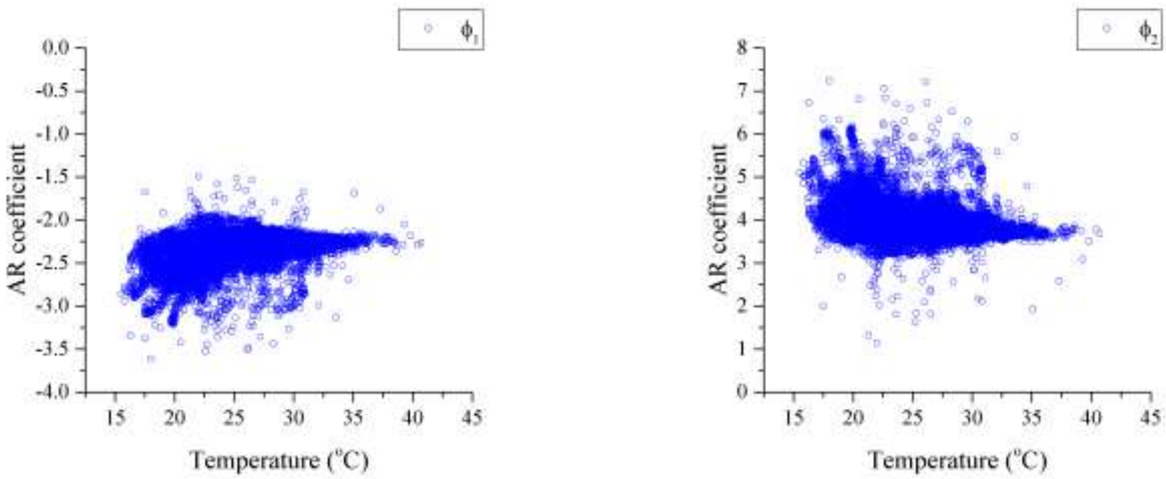

(a) φ_1 (b) φ_2

Fig. 14 First two AR model coefficient of acceleration vs. temperature

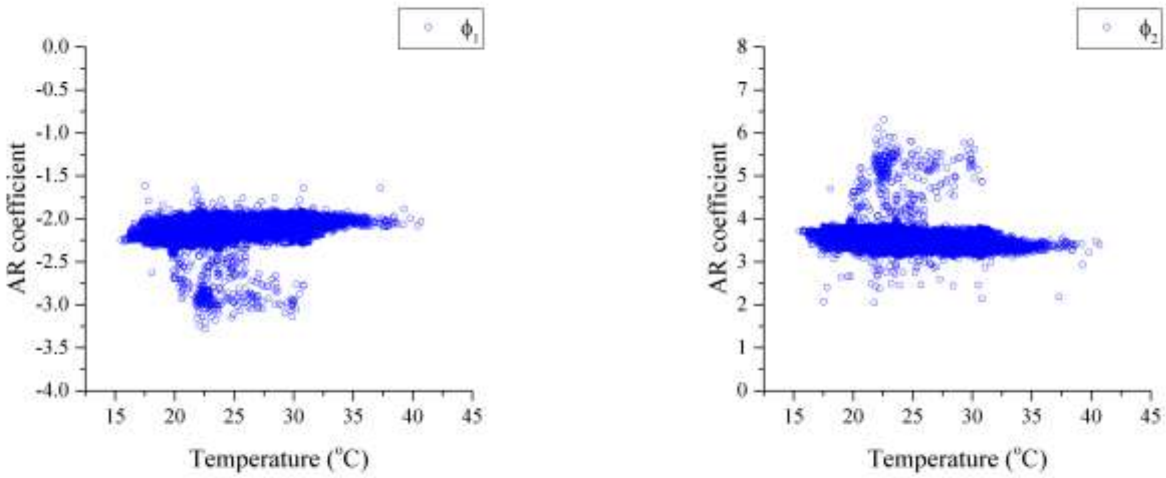

(a) φ_1 (b) φ_2

Fig. 15 First two AR model coefficients of inclination vs. temperature

of inclination and the temperature or wind speed. In Table 2, the correlation coefficients vary between -1 and 1, and the higher the absolute value of a correlation coefficient is, the stronger the correlation. A negative coefficient indicates a negative correlation, and a positive coefficient indicates a positive correlation.

As shown in Figs. 14 and 15, the absolute value of acceleration's AR model coefficients increases with the increase of temperature, while the inclination's AR model coefficients have a low correlation with temperature. The comparison of Figs. 14 and 15 validated the results in Table 2 as well.

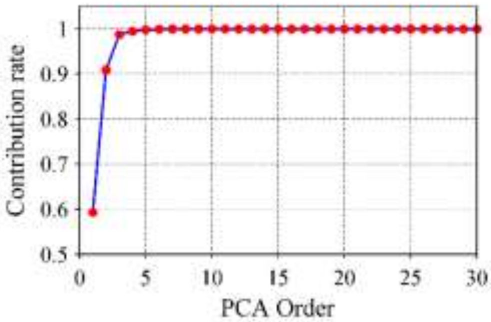

(a) acceleration

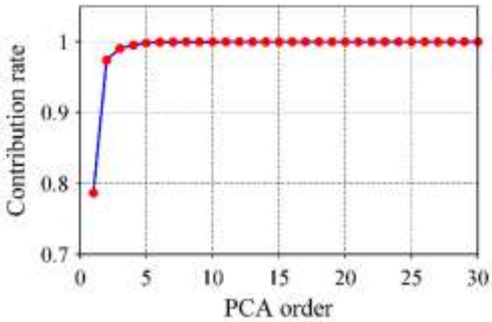

(b) inclination

Fig. 16 Cumulative contributions of the feature vectors of the AR model coefficients

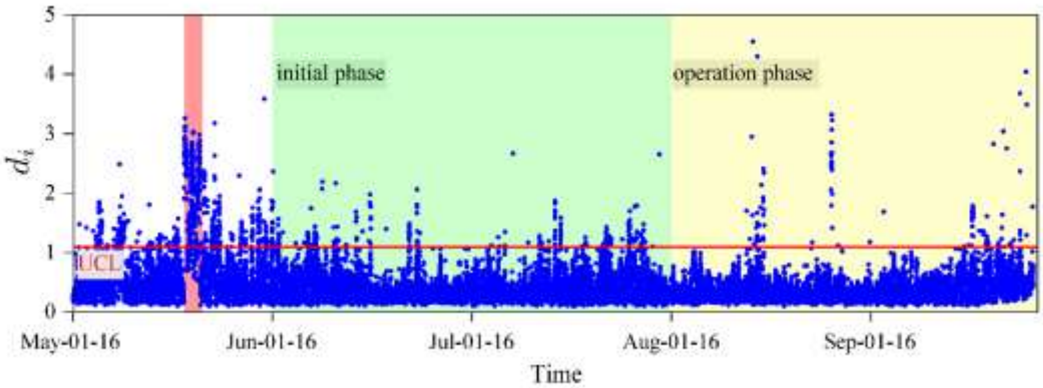

Fig. 17 Control chart of the PCA reconstruction error for the AR coefficients of acceleration data from the 117th floor

Table 3 Percentage of outliers in the control chart (%)

	Mid-May	*Week 1*	*Week 2*	*Week 3*	*Week 4*	*Week 5*	*Week 6*	*Week 7*	*Week 8*
Acceleration	69.5	0.0	3.0	0.0	2.7	0.3	0.0	4.2	3.0
Inclination	67.3	2.3	5.7	1.7	1.7	2.4	3.3	7.7	4.9

4.2 Principal component analysis

In May, a damper test of the Shanghai Tower was performed, and the damper was locked during the test period, which resulted in changes in the structural state. Therefore, the AR model coefficients in June and July were selected to obtain the principal components in the reference state. The cumulative variance contribution of the feature vectors of acceleration and inclination in the X direction on the 117th floor are shown in Fig. 16. According to the 95% cumulative variance contribution, the first three and the first two feature vectors of acceleration and inclination are selected as principal components. Using the obtained principal components, the AR model coefficients are reconstructed, and the Euclidean distance of the obtained reconstruction error vector is used as a structural state indicator.

4.3 Novelty detection

According to the statistics of the AR model parameter reconstruction error in June and July, the value corresponding to 95% of the cumulative probability distribution is determined as the UCL, and the points that exceed the UCL are defined as outliers. Therefore, the percentage of the outliers in the normal structural state is approximately 5%.

As shown in Figs. 17 and 18, during the damper test, the reconstruction errors of acceleration and inclination exhibit obvious anomalies, and the percentage of outliers during the damper test reaches 69.5% and 67.3%, respectively, indicating that the method can successfully identify the changes in the structural state. For the data from August and September, the percentage of outliers is calculated weekly, and the statistical results are shown in Table 3. The maximum weekly percentage of outliers in the two months

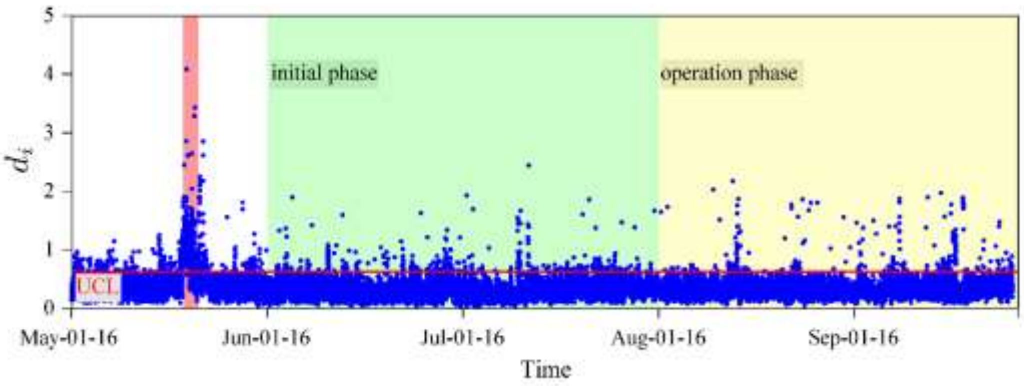

Fig. 18 Control chart of the PCA reconstruction error for the AR coefficients of inclination data from the 117th floor

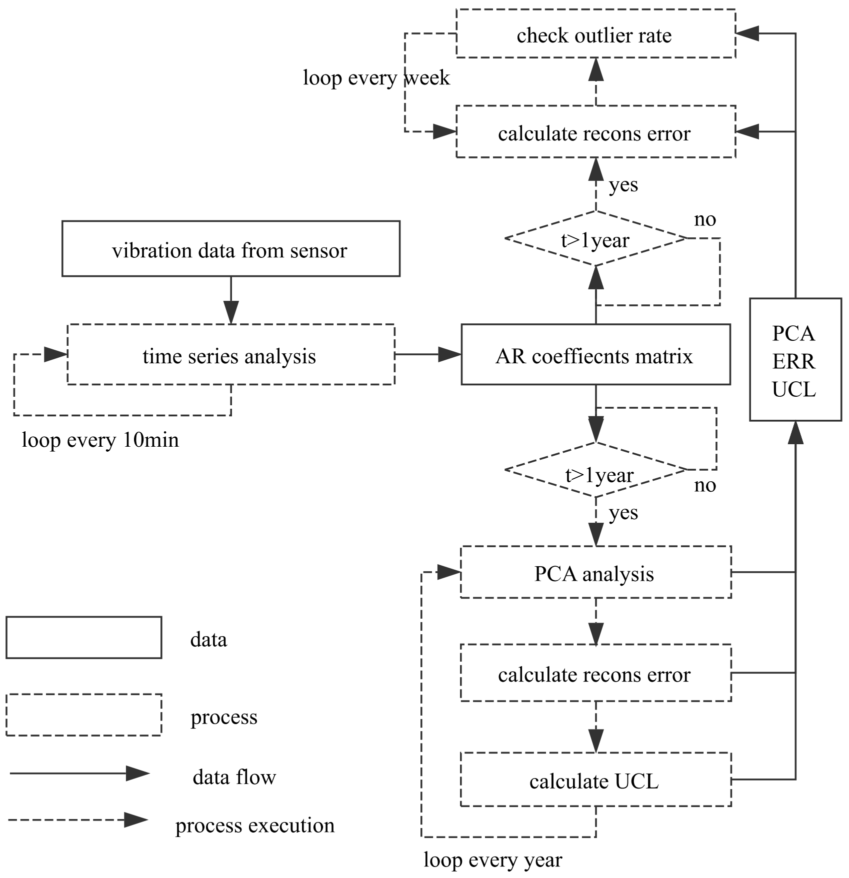

Fig. 19 Online automatic structural health assessment plan for the Shanghai Tower

is 7.7%, which means that in reference to June and July, the state of the structure does not change significantly.

The above analysis of the monitoring data indicates that the structural health assessment method proposed in this paper is suitable for the Shanghai Tower and can provide an early warning regarding structural state changes. A detailed plan for evaluating the health status of the Shanghai Tower and providing early warnings is proposed in the following section.

4.4 Online automatic structural health assessment plan for the Shanghai Tower

The online automatic structural health assessment plan for the Shanghai Tower is divided into two phases: the initial data accumulation phase and the structural health assessment system operation phase. The initial data accumulation phase lasts for one year to fully consider the effects of environmental factors. During the initial data accumulation phase, the principal components of the AR model coefficients and UCL values of reconstruction errors are determined and will be used in the operation phase. In the operation phase, the principal components of the AR model and UCL values of reconstruction errors are periodically (such as once a year) updated to consider the long-term changes in the structural state due to the factors such as the aging of materials and environmental erosion. The specific implementation of the online automatic structural health assessment plan is presented in Fig. 19.

5. Conclusions

In this article, the Shanghai Tower is introduced in detail, including the architectural and structural forms, the SHM system, and the dynamic characteristics obtained by AVT and FEM. Then, an online automatic structural health assessment method based on time series analysis, PCA and the control chart method is proposed. Finally, the proposed online automatic structural health assessment method is applied to analyze the acceleration and inclination data from the Shanghai Tower. The main conclusions of the paper are as follows.

Based on the data collected at Shanghai Tower, the average correlation coefficient between AR model coefficient of acceleration and temperature is 0.17 and the average correlation coefficient between AR model coefficient of inclination and temperature is 0.10, which indicates that acceleration's AR model coefficients are more sensitive to temperature.

During the damper test of the Shanghai Tower, the damper was locked, which led to changes in the state of the structure. In addition, the state change was clearly reflected by a shift in the time history curves of the inclination data and corresponding AR model coefficients. However, there was no obvious shift in the time history curves of the acceleration data and corresponding AR model parameters.

For the inclination and acceleration data, the control charts of the reconstruction error of the AR model coefficients displayed obvious shifts during the damper test period, and the percentage of outliers reached 67.3% and 69.5%, respectively. This result indicated that the reconstruction error of the AR model coefficients can effectively reflect a change in the structural state.

In the control charts of the reconstruction errors of AR model coefficients, the UCL was determined based on data from June and July. The control charts show that in August and September, most of the reconstruction error values were below the UCL and that the weekly percentage of outliers for both inclination and acceleration was less than 10%. Therefore, we can consider the Shanghai Tower to be in a healthy state.

Acknowledgments

The research described in this paper was financially supported by the National Natural Science Fund of China (NSFC) (grant No. 51878475) and the Natural Science Foundation of Shanghai (grant No. 16ZR1438900). The financial support is gratefully acknowledged. Special thanks to Hong Kong Polytechnic University and Tongji Architectural Design (Group) Co. Ltd for their contribution in the construction of the structural health monitoring system of the Shanghai Tower.

References

Abdelrazaq, A., Bentz, A., Kijewski-Correa, T., Guo, Y., Kwon, D.K., Kareem, A. and Bobby, S. (2013), "SmartSync: An integrated real-time structural health monitoring and structural identification system for tall buildings", *J. Struct. Eng.*, **139**(10), 1675-1687. https://doi.org/10.1061/(ASCE)ST.1943-541X.0000560.

Akaike, H. (1973), "Maximum likelihood identification of Gaussian autoregressive moving average models", *Biometrika*, **60**(2), 255-265. https://doi.org/10.1093/biomet/60.2.255.

Cornwell, P., Farrar, C.R., Doebling, S.W. and Sohn, H. (1999), "Environmental variability of modal properties", *Exp. Techniques*, **23**(6), 45-48. https://doi.org/10.1111/j.1747-1567.1999.tb01320.x.

de Lautour, O.R. and Omenzetter, P. (2010), "Damage classification and estimation in experimental structures using time series analysis and pattern recognition", *Mech. Syst. Signal Pr.*, **24**(5), 1556-1569. https://doi.org/10.1016/j.ymssp.2009.12.008.

Ding, J.M., Chao, S., Zhao, X., and Wu, H.L. (2010), "Critical issues of structural analysis for the Shanghai Center project", *J. Build. Struct.*, **31**(6), 122-131. (In Chinese)

Jolliffe, I. (2011), *Principal component analysis*, Springer, Berlin, Heidelberg, Germany.

Liu, T., Yang, B. and Zhang, Q. (2016), "Health monitoring system developed for Tianjin 117 high-rise building", *J. Aerosp. Eng.*, **30**(2), B4016004. https://doi.org/10.1061/(ASCE)AS.1943-5525.0000602.

Lu, Y. and Gao, F. (2005), "A novel time-domain auto-regressive model for structural damage diagnosis", *J. Sound Vib.*, **283**(3-5), 1031-1049. https://doi.org/10.1016/j.jsv.2004.06.030.

Magalhães, F., Cunha, Á. and Caetano, E. (2009), "Online automatic identification of the modal parameters of a long span arch bridge", *Mech. Syst. Signal Pr.*, **23**(2), 316-329. https://doi.org/10.1016/j.ymssp.2008.05.003.

Nair, K.K., Kiremidjian, A.S. and Law, K.H. (2006), "Time series-based damage detection and localization algorithm with application to the ASCE benchmark structure", *J. Sound Vib.*, **291**(1-2), 349-368. https://doi.org/10.1016/j.jsv.2005.06.016.

Ni Y.Q., Xia Y., Liao W.Y. and Ko J.M. (2009), "Technology innovation in developing the structural health monitoring system for Guangzhou New TV Tower", *Struct. Control Health Monit.*, **16**(1), 73-98. https://doi.org/10.1002/stc.303.

Peeters, B. and De Roeck, G. (2001), "One-year monitoring of the Z24-Bridge: environmental effects versus damage events", *Earthq. Eng. Struct. D.*, **30**(2), 149-171. https://doi.org/10.1002/1096-9845(200102)30:2<149::AID-EQE1>3.0.CO;2-Z

Posenato, D., Lanata, F., Inaudi, D. and Smith, I.F.C. (2008), "Model-free data interpretation for continuous monitoring of complex structures", *Adv. Eng. Inform.*, **22**(1), 135-144. https://doi.org/10.1016/j.aei.2007.02.002.

Reynders, E., Houbrechts, J. and De Roeck, G. (2012), "Fully automated (operational) modal analysis", *Mech. Syst. Signal Pr.*, **29**, 228-250. https://doi.org/10.1016/j.ymssp.2012.01.007.

Shi, W., Shan, J. and Lu, X. (2012), "Modal identification of Shanghai World Financial Center both from free and ambient vibration response", *Eng. Struct.*, **36** 14-26. https://doi.org/10.1016/j.engstruct.2011.11.025.

Sohn, H. and Farrar, C.R. (2001), "Damage diagnosis using time series analysis of vibration signals", *Smart Mater. Struct.*, **10**(3), 446-451.

Su, J., Xia, Y., Chen, L., Zhao, X., Zhang, Q., Xu, Y., Ding, J., Xiong, H., Ma, R. and Lv, X. (2013), "Long-term structural performance monitoring system for the Shanghai Tower", *J. Civil Struct. Health Monit.*, **3**(1), 49-61.

Ubertini, F., Comanducci, G. and Cavalagli, N. (2016), "Vibration-based structural health monitoring of a historic bell-tower using output-only measurements and multivariate statistical analysis", *Struct. Health Monit.*, **15**(4), 438-457. https://doi.org/10.1177/1475921716643948.

Ubertini, F., Gentile, C. and Materazzi, A.L. (2013), "Automated modal identification in operational conditions and its application to bridges", *Eng. Struct.*, **46**, 264-278. https://doi.org/10.1016/j.engstruct.2012.07.031.

Yan, A.M., Kerschen, G., De Boe, P. and Golinval, J.C. (2005a), "Structural damage diagnosis under varying environmental conditions—Part I: A linear analysis", *Mech. Syst. Signal Pr.*, **19**(4), 847-864. https://doi.org/10.1016/j.ymssp.2004.12.002.

Yan, A.M., Kerschen, G., De Boe, P. and Golinval, J.C. (2005b), "Structural damage diagnosis under varying environmental conditions—part II: local PCA for non-linear cases", *Mech. Syst. Signal Pr.*, **19**(4), 865-880. https://doi.org/10.1016/j.ymssp.2004.12.003.

Yi, T., Li, H. and Zhang, X. (2015), "Health monitoring sensor placement optimization for Canton Tower using virus monkey algorithm", *Smart Struct. Syst.*, **15**(5), 1373-1392. http://dx.doi.org/10.12989/sss.2015.15.5.1373.

Zhang, Q., Yang, B., Liu, T., Li, H. and Lv, J. (2015), "Structural health monitoring of Shanghai tower considering time-dependent effects", *Int. J. High-Rise Build.*, **4**(1), 39-44.

HJ